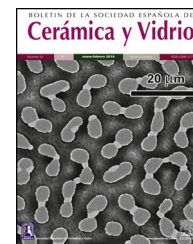




BOLETIN DE LA SOCIEDAD ESPAÑOLA DE
Cerámica y Vidrio

www.elsevier.es/bsecv



Original

Enzyme immobilization using two processing methods onto silica core-shell particles



Milan P. Nikolić^{a,*}, Vladimir B. Pavlović^b, Slobodanka Stanojević-Nikolić^a,
 Vladimir V. Srdić^c

^a Department of Chemistry and Chemical Engineering, Faculty of Agronomy, Čačak, University of Kragujevac, Serbia

^b Faculty of Agriculture, University of Belgrade, Department of Agricultural Engineering, Nemanjina 6, 11080 Zemun, Serbia

^c Department of Materials Engineering, Faculty of Technology, University of Novi Sad, Serbia

ARTICLE INFO

Article history:

Received 13 September 2019

Accepted 11 March 2020

Available online 18 April 2020

Keywords:

Silica

Core-shell particles

Mesoporous

Lipase

Invertase

Immobilization

ABSTRACT

Two methods of enzyme immobilization onto silica core-shell particles were developed. The first method involved the immobilization of *Candida rugosa* lipase inside a previously synthesized mesoporous silica layer (deposited at 80 °C) surrounding a dense silica core. To prevent lipase leakage from the support, an outer mesoporous silica layer was deposited at 40 °C around the first silica layer containing the immobilized lipase. The deposition of the second layer was performed at a relatively lower temperature, to prevent thermal inactivation of the immobilized enzyme. The internal silica layer was obtained by assembling primary silica nanoparticles generated from highly basic sodium silicate solution at 80 °C on the surface of poly (diallyldimethylammonium chloride) (PDDA) functionalized silica core particles. The average shell thickness and pore size of the internal silica layer was ~60 nm and 24 nm, respectively. The effect of process parameters on generation and aggregation of silica nanoparticles prepared from highly basic sodium silicate solution was also investigated. The aggregation of silica particles generated at 40 °C and 80 °C took place after 840 s and 570 of reactions, respectively. The immobilization efficiency of lipase on the mesoporous silica monolayer was 80%. A decline of immobilized lipase activity was approximately 6 times after 10 reaction cycles due to lipase leakage from the monolayered shell. An outer mesoporous silica layer was deposited at 40 °C onto the surface of previously PDDA-functionalized monolayered silica core-shell particles containing the immobilized lipase. The average thickness and pore size of outer mesoporous silica layer was ~60 nm and 17 nm, respectively. The activity of lipase immobilized inside the bilayered shell was further reduced due to diffusion resistance within the outer silica layer and PDDA layer however, it was retained for the next reaction cycles.

The pore size of mesoporous silica layer obtained at 80 °C was insufficient to allow invertase immobilization. Thus, the second method for the immobilization of invertase was developed. It involved the preparation of the mesoporous silica layer simultaneously with

* Corresponding author.

E-mail address: milanik@kg.ac.rs (M.P. Nikolić).

<https://doi.org/10.1016/j.bsecv.2020.03.004>

0366-3175/© 2020 SECV. Published by Elsevier España, S.L.U. This is an open access article under the CC BY-NC-ND license (<http://creativecommons.org/licenses/by-nc-nd/4.0/>).

invertase immobilization at 40 °C. The immobilized invertase showed decreased activity, but it was not hampered by substrate inhibition, as in the case of the free enzyme, due to the location of the enzyme inside the mesoporous silica layer, where the mass transfer resistance for the substrate to the enzyme active site was present.

© 2020 SECV. Published by Elsevier España, S.L.U. This is an open access article under the CC BY-NC-ND license (<http://creativecommons.org/licenses/by-nc-nd/4.0/>).

Inmovilización enzimática usando dos métodos de procesamiento en partículas de núcleo-cubierta de sílice

R E S U M E N

Palabras clave:

Sílice
Partículas núcleo-cubierta
Mesoporosa
Lipasa
Invertasa
Inmovilización

Han sido desarrollados dos métodos de inmovilización enzimática sobre las partículas de la núcleo-cubierta de sílice. El primer método implicaba la inmovilización de *Candida rugosa* lipasa dentro de una capa de sílice mesoporosa previamente sintetizada (depositada a 80 °C), la cual rodea un núcleo denso de sílice. Para evitar fugas de la lipasa del soporte, se depositó una capa externa mesoporosa de sílice a una temperatura de 40 °C sobre la superficie de las partículas de la núcleo-cubierta de sílice que contenían la lipasa inmovilizada. La deposición de la segunda capa se realizó a una temperatura relativamente más baja para evitar la inactivación térmica de la enzima inmovilizada. La capa interna de sílice se obtuvo ensamblando nanopartículas de sílice primaria generadas a partir de una solución de silicato de sodio altamente básica a 80 °C en la superficie de las partículas del núcleo de sílice funcionalizadas con poli (cloruro de dialildimetilamonio) (PDDA). El grosor medio de la cubierta y el tamaño de poro de la capa interna de sílice fue de ~60 nm y 24 nm, respectivamente. También se investigó el efecto de los parámetros del proceso sobre la generación y agregación de las nanopartículas de sílice preparadas a partir de una solución de silicato de sodio altamente básica. La agregación de las partículas de sílice generadas a 40 °C y 80 °C tuvo lugar después de 840 s y 570 s de reacción, respectivamente. La eficiencia de la inmovilización de la lipasa en la monocapa de sílice mesoporosa fue del 80%. La disminución de la actividad de la lipasa inmovilizada fue de aproximadamente 6 veces después de 10 ciclos de reacción debido a la fuga de la lipasa de la cubierta monocapa. Se depositó una capa de sílice mesoporosa externa a 40 °C sobre la superficie de las partículas de la núcleo-cubierta de sílice monocapa previamente estratificadas de PDDA que contenían la lipasa inmovilizada. El grosor promedio y el tamaño de los poros de la capa de sílice mesoporosa externa fue de ~60 nm y 17 nm, respectivamente. La actividad de la lipasa inmovilizada dentro de la cubierta bicapa se redujo aún más debido a la resistencia a la difusión dentro de la capa de sílice externa y la capa de PDDA y, sin embargo, se retuvo para los siguientes ciclos de reacción.

El tamaño de poro de la capa de sílice mesoporosa obtenida a 80 °C fue insuficiente para permitir la inmovilización de la invertasa. Así, El segundo método para la inmovilización de la invertasa fue desarrollado debido a que la invertasa era mayor que el poro de la capa de sílice mesoporosa previamente sintetizada. Lo mismo implicaba la preparación de la capa de sílice mesoporosa simultáneamente con la inmovilización de la invertasa a una temperatura de 40 °C. La invertasa inmovilizada mostró una actividad disminuida, pero no fue obstaculizada por la inhibición del sustrato, como en el caso de la enzima libre, debido a la ubicación de la enzima dentro de la capa de sílice mesoporosa, donde existía resistencia a la transferencia de masa del sustrato a la enzima activa.

© 2020 SECV. Publicado por Elsevier España, S.L.U. Este es un artículo Open Access bajo la licencia CC BY-NC-ND (<http://creativecommons.org/licenses/by-nc-nd/4.0/>).

Introduction

Enzymes are versatile biocatalysts used in processes for production of a wide variety of fine chemicals [1], medicines [2] and biosensors [3]. Enzyme-catalyzed reactions are environmentally friendly [4], but enzymes have high activity and selectivity under relatively mild reaction conditions.

However, under extreme conditions (high temperatures, extreme pH, organic solvents), enzymes are easily inactivated due to denaturation. Moreover, the application of natural enzymes is hampered by difficulties in reuse, product contamination and separation. The approach taken to resolve these difficulties is to immobilize enzymes onto solid supports, in order to enable their reuse and the formation of stable heterogeneous biocatalysts. As a result of their excellent

properties, such as adjustable size, morphology and porosity, along with their chemical stability, biocompatibility and non-toxicity, mesoporous silica particles have widely been used for enzyme immobilization [5,6]. In recent years, silica core-shell particles (solid core-porous shell or superficially porous particles) have demonstrated a wide range of applications, including separation [7], drug delivery [8], chemical catalysis [9] and enzyme immobilization [10]. Uniform silica core particles are often synthesized by the Stöber process [11] which is based on hydrolysis and condensation of highly reactive tetraethylortosilicate (TEOS) precursor catalyzed by ammonia with water in low molecular weight alcohol. In addition, it has been shown [11–13] that size and distribution of the synthesized silica particles are very sensitive to the TEOS:NH₄OH:H₂O molar ration and TEOS concentration.

The formation of mesoporous silica layers around silica cores is mainly based on the use of surfactants that are aggregated on the surface of silica cores, followed by condensation of TEOS on the surface of modified cores [8–10]. In these cases, calcination or extraction is performed to remove the template from the structure. The different silica coating thicknesses can be prepared by varying the core/TEOS ratio in the initial suspensions as it was found for the precipitation of silica onto the surface of previously obtained alumina cores [15]. The neutralization of sodium silicate solution induces nucleation of silica nanoparticles, which aggregate to form particles with mesoporous structures [10]. Therefore, mesoporous silica shells can be synthesized without templates by a simple procedure involving the electrostatic deposition of silica nanoparticles prepared from highly basic sodium silicate solution on the surface of functionalized cores [16,17]. The use of a cationic polyelectrolyte layer on the surface of core particles improved the electrostatic deposition of precipitated silica and the formation of uniform and continuous silica layers [16,18].

The growing interest in processes with the use of immobilized enzymes leads to the development of new supports suitable for enzyme immobilization. Thus, the design and characterization of new supports as well as the methods for enzyme immobilization have been increasingly valued. In this research, two processing methods for the immobilization of lipase and invertase onto silica core-shell structures were developed. The reason was the different sizes of these two enzymes. *Candida rugosa* lipase has an apparent molecular weight of 60 kDa [19] and a molecular volume of $5 \times 4.2 \times 3.3 \text{ nm}^3$ [20] while invertase from *Saccharomyces cerevisiae* has a molecular weight of 270 kDa [21]. Bilayered silica core-shell structures were developed for lipase immobilization while monolayered silica core-shell particles were developed for invertase immobilization.

Experimental

Bilayered silica core-shell particles containing immobilized lipase were prepared using a three-step process. In the first step, silica core particles were synthesized by the hydrolysis and condensation of tetraethylortosilicate (TEOS) by the Stöber process [11] and functionalized with poly(diallyldimethylammonium chloride) (PDDA). In the second step, a mesoporous silica layer was prepared by the

deposition of silica nanoparticles generated by the neutralization of highly basic sodium silicate solution on the surface of the previously synthesized positively charged silica core particles. The as-synthesized silica core-shell particles were used as a host for lipase immobilization. In the third step, an outer mesoporous silica layer was deposited on the surface of the silica core-shell particles containing the immobilized enzymes to prevent enzyme leakage from the support.

Monolayered silica core-shell particles containing immobilized invertase were prepared by a two-step process. In the first step, silica core particles were prepared from TEOS and functionalized with PDDA. In the second step, a mesoporous silica layer containing immobilized invertase was prepared by dispersing functionalized silica core particles in an aqueous solution containing invertase and sodium silicate. The mesoporous silica layer with the entrapped enzyme was deposited on the surface of positively charged silica core particles.

Synthesis of silica core particles

Silica core particles (sample C) were synthesized by the hydrolysis and condensation of tetraethylortosilicate (TEOS), dissolved in anhydrous ethanol, with distilled water under basic condition (25% NH₃, Merck). The sample was prepared by the Stöber process using a molar ratio of TEOS:H₂O:NH₄OH = 1:40:2 and a TEOS concentration of 0.25 mol/l [16]. After feeding, the product suspension was continuously stirred at room temperature for 1 h. The white precipitated powder was centrifuged and washed with distilled water until the pH of effluent was approximately 7, and finally dried at 120 °C for 1 day.

Preparation of the first mesoporous silica layer with immobilized lipase

In order to enable the electrostatic assembly of primary silica nanoparticles on silica core particles (sample C), their surfaces were functionalized with poly(diallyldimethylammonium chloride) (PDDA) (Fig. 1a). PDDA-functionalized silica particles (sample C_P) were prepared by suspending silica core particles (1.5 g) in 70 ml PDDA solution (at a concentration of 12 mg/ml), which also contained 0.05 M NaCl [16]. The obtained suspension was stirred for 20 min at 70 °C, and the functionalized particles (sample C_P) were centrifuged, washed with distilled water, and finally dried at 100 °C.

The first mesoporous silica layer (with somewhat larger pores) was prepared by the deposition of silica nanoparticles generated by the neutralization of highly basic sodium silicate solution on the surface of the previously synthesized positively charged PDDA-functionalized silica core particles [16]. The PDDA-functionalized SiO₂ core particles were dispersed in highly basic sodium silicate solution (Water Glass, Birač Alumina Factory, Zvornik) having a Na₂O/SiO₂ molar ratio of 0.4 and a SiO₂ concentration of 1.25 mol/l (Fig. 1b). Sulfuric acid (1 mol/l) was slowly added to a well-stirred sodium silicate solution (containing dispersed PDDA-functionalized SiO₂ core particles) at 80 °C to decrease the pH value and enable particulate silica layer formation. The optimum reaction temperature and time were selected for the preparation of an appropriate mesoporous structure for enzyme immobilization (Fig. 1c). When the reaction finished, the obtained particles (sample

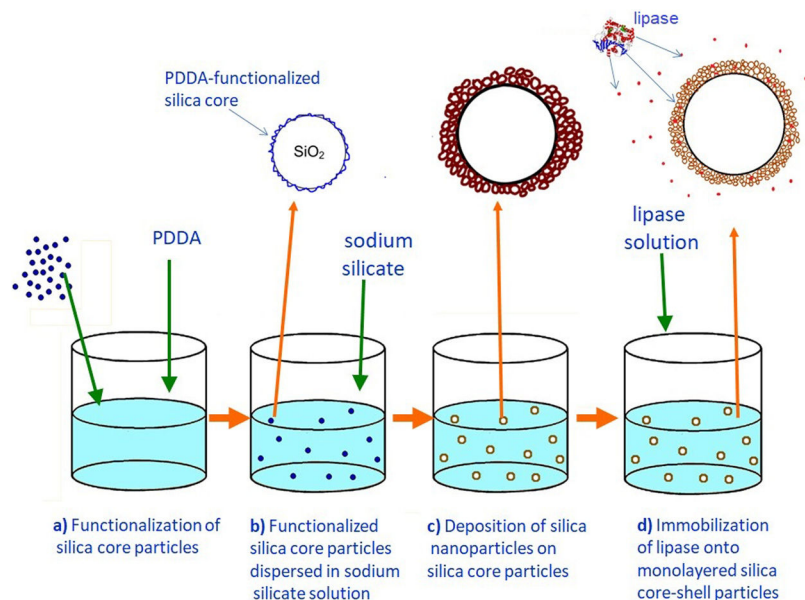


Fig. 1 – Preparation scheme of the first mesoporous silica layer with immobilized lipase.

C_PS) were separated from the liquid phase by centrifugation, washed with distilled water, and finally dried at 120 °C for one day.

The immobilization of lipase from *C. rugosa* (Sigma–Aldrich) onto the mesoporous silica layer was performed according to the following procedure: 1.3 g of as-synthesized silica core-shell particles and 100 ml of lipase solution (0.065 mg/ml) in phosphate buffer (0.05 M and pH=7.0) were added to a flask and stirred magnetically for 1 h at ambient temperature (Fig. 1d). The reaction mixture was centrifuged and the supernatant was used for the determination of the amount of lipase remaining in the solution. The concentration of lipase solution was measured by the Bradford method [20], with BSA (bovine serum albumin) as a standard at 595 nm. A similar procedure was used for the immobilization of invertase from baker's yeast (*S. cerevisiae*) (Sigma–Aldrich) onto the mesoporous silica layer, but it was unsuccessful.

Formation of an outer silica layer around lipase-immobilized silica core-shell particles

An outer mesoporous silica layer (with somewhat smaller pores) was deposited on the surface of silica core-shell particles containing the immobilized lipase to prevent enzyme leakage from the support. To achieve the electrostatic assembly of silica nanoparticles on the surface of the previously obtained enzyme-immobilized silica core-shell particles, the latter were functionalized with PDDA (Fig. 2a). The PDDA-functionalized lipase-immobilized silica particles were prepared by dispersing 1.3 g of enzyme-immobilized silica particles in 50 ml PDDA solution (at a concentration of 12 mg/ml), which also contained 0.05 M NaCl. The suspension was stirred for 20 min at room temperature. The modified particles (sample C_PS_P) were centrifuged and successively washed with distilled water.

The PDDA-functionalized silica core-shell particles containing the immobilized lipase were used as templates for assembling an external silica layer. These particles were dispersed in highly basic sodium silicate solution having a Na₂O/SiO₂ molar ratio of 0.4 and a SiO₂ concentration of 1.25 mol/l (Fig. 2b). Sulfuric acid (1 mol/l) was slowly added to this well-stirred dispersion at 40 °C to decrease the pH value and enable the generation of silica nanoparticles and their deposition on the surface of the PDDA-functionalized lipase-immobilized silica particles (Fig. 2c). The optimum reaction temperature and time were selected for the preparation of an appropriate mesoporous structure to prevent enzyme (lipase) leakage from the support. When the reaction finished, the obtained particles (sample C_P-S_P-S) were separated from the liquid phase by centrifugation, washed with distilled water, and finally dried at room temperature.

Preparation of a mesoporous silica layer simultaneously with invertase immobilization

The PDDA-functionalized SiO₂ core particles were dispersed in highly basic sodium silicate solution having a Na₂O/SiO₂ molar ratio of 0.4 and a SiO₂ concentration of 1.25 mol/l. Sulfuric acid (1 mol/l) was slowly added to the well-stirred dispersion at 40 °C, to decrease the pH value and enable the generation of silica nanoparticles. A small aliquot of invertase (from baker's yeast *S. cerevisiae*, Sigma–Aldrich) solution (2 ml at a concentration of 0.178 mg/ml) was added to the reaction vessel before the gel point was reached. The reaction lasted for 2 min and was stopped when the gel point was reached. The white precipitated powder was centrifuged, washed with distilled water, and finally dried at room temperature for 2 days. Viscosity variation of silica sols with neutralization time and the moment of reaching the gel-point were obtained by neutralization of highly basic sodium silicate solution (having

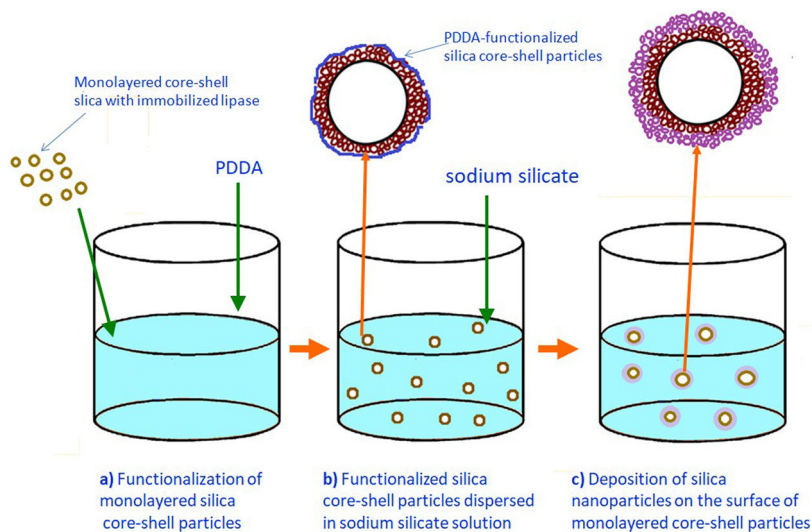


Fig. 2 – Preparation scheme of an outer silica layer around lipase-immobilized silica core-shell particles.

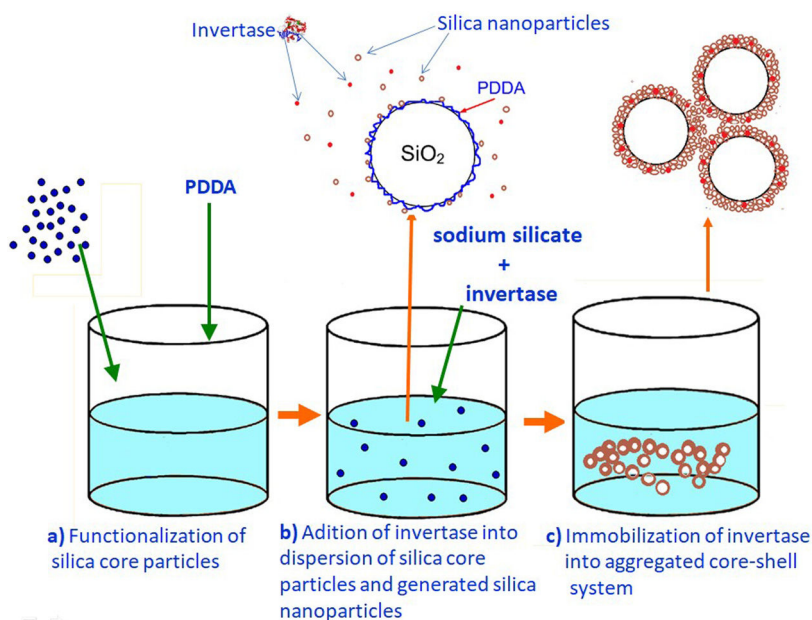


Fig. 3 – Preparation scheme of a mesoporous silica layer simultaneously with invertase immobilization.

a $\text{Na}_2\text{O}/\text{SiO}_2$ molar ratio of 0.28 and a SiO_2 concentration of 0.91 mol/l) at 70°C (Fig. 3).

Characterization of silica particles

Particle size and zeta potential were measured by dynamic light scattering (Zetasizer Nano ZS, Malvern Instruments). The size and morphology of the particles were examined using a scanning electron microscope (JEOL JSM 6460 LV) operating at 20 kV. Prior to SEM imaging, the samples were sputtered with gold. TEM characterization was performed using a JEM 1400-Plus JEOL device operating at 120 kV.

The specific surface area (according to the BET method) [23], pore size distribution (according to the BJH method) [24] and pore volume of as-synthesized silica particles were measured by low-temperature nitrogen adsorption using a

Quantachrom Autosorb-3B instrument. The samples were outgassed at 150°C for 12 h under a vacuum of 10^{-4} Pa prior to the adsorption measurements.

The viscosity vs. shear-rate relations for silica sols obtained by neutralization of highly basic sodium silicate solution were measured by HAAKE RheoStress 600.

Activity assay of free and immobilized enzymes

The immobilization efficiency (%) of the enzyme was calculated using the equation:

$$\text{Immobilization efficiency} = \frac{C_i - C_f}{C_i} \times 100$$

where C_i and C_f are the initial and final concentration of the enzyme, respectively.

The activities of the free and immobilized lipase were measured by monitoring the catalytic hydrolysis of 4-nitrophenyl acetate (pNPA) into 4-nitrophenol [25]. Due to poor solubility in water, pNPA was first dissolved in acetonitrile and then dropwise added to the phosphate buffer (0.05 M, pH=7). The effect of temperature on the activity of native lipase was performed by adding 400 μ l of free enzyme solution (at a concentration of 0.03 mg/ml) to 10 ml of lipase substrate (the concentration of 4-nitrophenyl acetate was 0.55 mM) at 30, 38, 46, 54 and 62 °C, respectively. Enzymatic activity was calculated based on three assays at each temperature. Activity assays were carried out by adding 400 μ l of free enzyme solution (at a concentration of 0.03 mg/ml) or 150 mg of the enzyme-loaded material (the amount of bound enzyme on support C_PS and C_P-S_P-S was 6 and 4 mg per gram of support, respectively) to 10 ml of lipase substrate (the concentration of 4-nitrophenyl acetate was 1.1 mM) at 25 °C. Due to diffusion limitations, the reaction time of the immobilized lipase was prolonged (the reaction time of the free and immobilized lipase was 2 and 15 min, respectively). Afterwards, the amount of 4-nitrophenol was determined spectrophotometrically at 410 nm. Both negative and positive controls were studied. The positive control was the reaction mixture to which the free or immobilized enzyme was added at the beginning of the reaction time. The negative control contained no enzyme.

The activities of the free and immobilized invertase were determined in measurements of reducing sugars produced by the enzymatic hydrolysis of sucrose into glucose and fructose. These activity assays were performed by adding 50 μ l of the free enzyme in acetate buffer (at a concentration of 0.22 mg/ml and pH=4.5) or 0.5 g of the enzyme-loaded material to 10 ml of sucrose (having three concentrations 0.05, 0.1 and 0.2 M) in the same buffer. After exactly 30 min of incubation at 25 °C, the sample was placed in a test tube containing 3 ml of dinitrosalicylic acid reagent (DNS) [26]. The mixture was placed in boiled water for 5 min to develop a red-brown color. Subsequently, 1 ml of a 40% potassium sodium tartrate (Rochelle salt) solution was added to stabilize the color. After cooling to room temperature in a cold water bath, the mixture was diluted with 10 ml of water and finally the absorbance was recorded by a spectrophotometer at 575 nm. The calibration curve was based on previous measurements of invert standard solutions (an equimolar mixture of glucose and fructose) of known concentrations.

Results and discussion

Immobilization of lipase in the mesoporous silica core-shell structure

To determine an optimum reaction temperature and optimum time for the deposition of both mesoporous silica layers, the following items should be analyzed: (i) the size of *C. rugosa* lipase, (ii) the effect of temperature on the activity of native lipase and (iii) neutralization conditions of the sodium silicate solution.

C. rugosa lipase has a molecular volume of $5 \times 4.2 \times 3.3 \text{ nm}^3$ [19]. Therefore, the first silica layer, in which this enzyme is to be immobilized, should have relatively large mesopores.

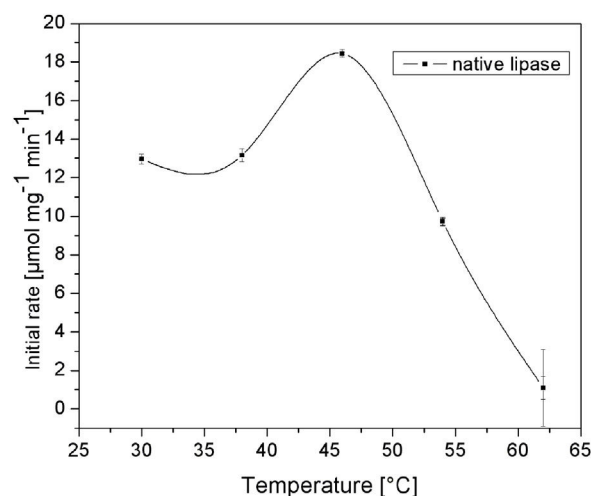


Fig. 4 – The effect of temperature on the activity of native lipase.

The effect of temperature on the activity of native lipase is shown in Fig. 4. It is obvious that native lipase is completely inactivated above 60 °C. Hence, the deposition of the second layer should be performed at a relatively lower temperature, to prevent thermal inactivation of the immobilized enzyme. According to these requirements and our previous results [16,17], two different temperatures (40 and 80 °C) and a reaction time of up to 840 s were investigated.

Fig. 5 shows particle size distributions of samples obtained by the neutralization of sodium silicate solution (having a SiO₂ concentration of 1.25 mol/l and a Na₂O/SiO₂ molar ratio of 0.4) at 40 and 80 °C. The samples were taken from the vessel during the reaction at different time intervals. Sulfuric acid was slowly added to the well-stirred sodium silicate solution, to keep the rate of neutralization constant at both temperatures. The increase in the average particle size with time was less pronounced at the lower temperature. A bimodal particle size distribution, with a high-intensity peak at $\sim 2 \text{ nm}$ and a smaller one at $\sim 9 \text{ nm}$, was observed after reaction at 40 °C for 480 s (Fig. 5a). The prolongation of the reaction led to an increase in primary particle size. However, after 840 s, the aggregation of silica particles resulted in the formation of very large particles of about 5 μm . Conversely, the increase in the average particle size with time was more pronounced at the higher temperature (Fig. 5b). It was also noted that the aggregation of the primary silica particles obtained at 80 °C took place after a shorter period of time (a small peak at $\sim 5 \mu\text{m}$ was observed as early as after 570 s) than in the case of the particles synthesized at 40 °C.

The nitrogen adsorption–desorption isotherms of silica particles obtained from sodium silicate solution at 40 and 80 °C are shown in Fig. 6. Both belong to Type IV, indicating that these particles have mesoporous structures. The average pore size distributions of silica particles obtained from sodium silicate solution at 40 and 80 °C are given in Fig. 6b, clearly showing that the average pore size of the obtained silica particles is ~ 17 and 24 nm, respectively (Table 1). On the other side, the average pore size of silica core particles was below 2 nm, indicating the microporous structure (Table 1). Additional information,

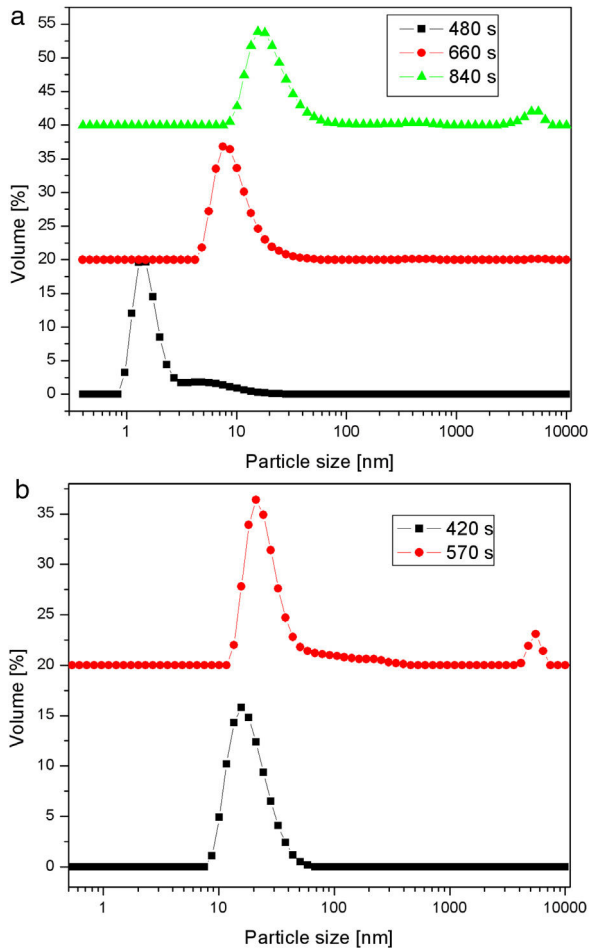


Fig. 5 – The average size of silica particles obtained by the acidic neutralization of highly basic sodium silicate solution at: (a) 40 °C and (b) 80 °C for different reaction times.

such as total pore volume and specific surface area, are also shown in Table 1. High surface area and very fine porosity of silica core particles correspond to a small size of primary particles obtained by hydrolysis and condensation of TEOS and their fractal structure [13]. As it was shown, an increase of temperature for the reaction of sodium silicate with sulfuric acid resulted in increasing of average pore size and decreasing of the specific surface area and the total pore volume. The reason for the observed differences lies in the fact that at low temperature reactions are slow and, thus, the primary particle size and concentration were small. Thus, the primary interparticle pores were smaller at lower temperature and specific surface area was higher. The total pore volume of silica particles generated at 80 °C was lower than that obtained at 40 °C. The higher temperature may have resulted in increasing

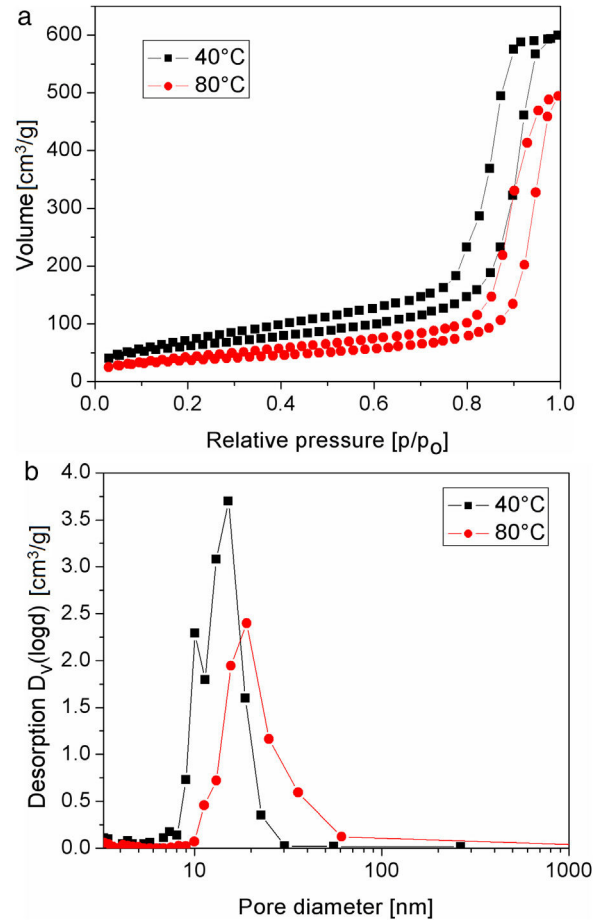


Fig. 6 – Adsorption-desorption isotherms (a) and pore size distribution (b) of silica particles synthesized by the neutralization of sodium silicate solution at 40 and 80 °C.

concentration of primary silica particles generated by neutralization of sodium silicate solution. Thus, aggregation of primary silica particles from concentrated silica sols resulted in a dense packing of primary particles and, consequently, the average pore volume of obtained mesoporous volume was decreased.

As shown by the results, the first silica layer with larger mesopores (Fig. 7) was deposited at 80 °C after a reaction time of 9 min, while the second silica layer with smaller mesopores (Fig. 7) was prepared at 40 °C after a reaction time of 12 min.

SEM micrographs of silica core particles and monolayered and bilayered silica core-shell particles are shown in Fig. 8. The silica core particles obtained from TEOS are spherical and monodispersed, with a smooth surface and the average particle size of about 400 nm (Fig. 8a). A rough surface of silica core-shell particles is clearly visible in the SEM micrographs

Table 1 – Specific surface area, total pore volume and average pore diameter of as-synthesized silica particles.

	Silica core particles (sample C)	Silica particles synthesized at 40 °C	Silica particles synthesized at 80 °C
Specific surface area [m ² /g]	324	218	127
Total pore volume [cm ³ /g]	0.186	0.927	0.764
Average pore diameter [nm]	<2	17	24

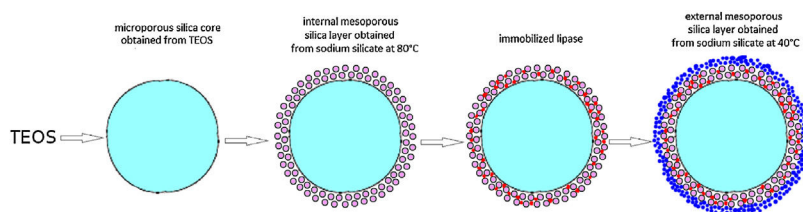


Fig. 7 – A schematic illustration of the preparation of bilayered silica core-shell particles containing immobilized enzymes.

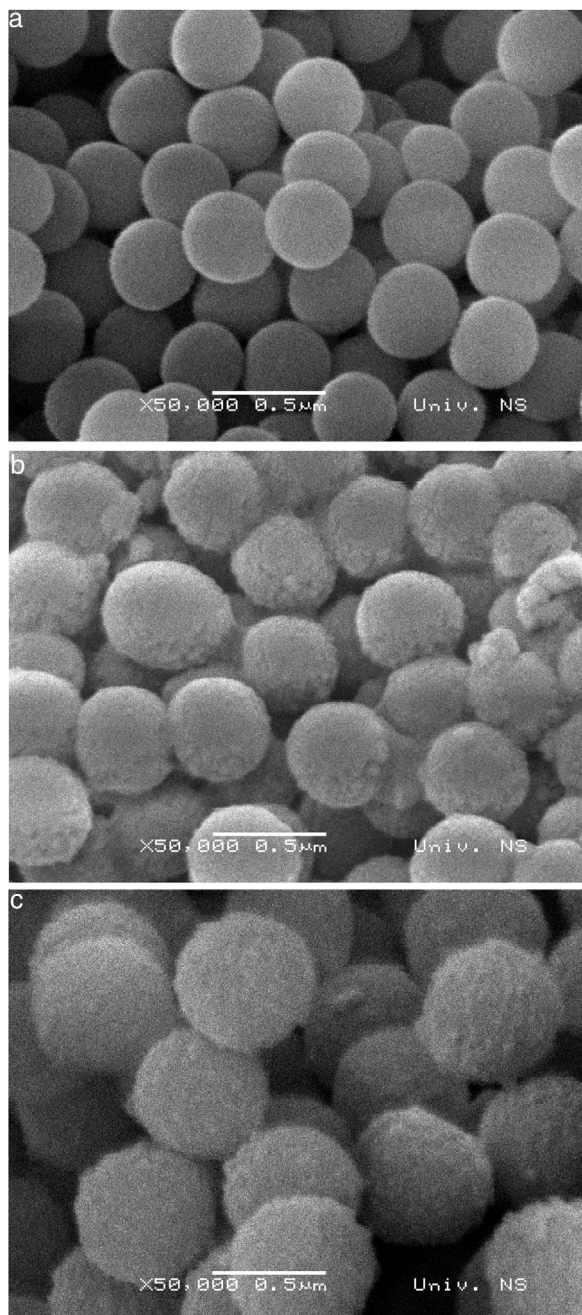


Fig. 8 – SEM images of: (a) silica core particles, (b) monolayered and (c) bilayered silica core-shell particles.

(Figs. 8b and c), indicating that the silica nanoparticles generated from sodium silicate solution were deposited on the surface of silica core particles. TEM micrographs of monolayered and bilayered silica core-shell particles are shown in Fig. 9. The obtained shells are continuous but slightly inhomogeneous. TEM micrograph revealed the average primary particle size of ~ 15 nm and porosity of mesoporous silica shell (Fig. 9a). The thickness of monolayered silica shell is around 60 nm, while the thickness of bilayered silica shell is ~ 120 nm (Fig. 9b).

The immobilization efficiency of lipase on the mesoporous silica layer (sample CpS) was 80%. When a similar procedure was used for the immobilization of invertase onto the mesoporous silica layer, the efficiency was 0%. *C. rugosa* lipase has an apparent molecular weight of 60 kDa [19] and a molecular volume of $5 \times 4.2 \times 3.3 \text{ nm}^3$ [20] while invertase from *S. cerevisiae* has a molecular weight of 270 kDa [21]. The average pore size of the mesoporous silica layer was 24 nm which allowed lipase immobilization within mesopores. However, the pore size was insufficient to allow invertase immobilization, indicating that another procedure should be used for the immobilization of invertase onto mesoporous silica.

The zeta potential of non-functionalized silica core particles (sample C) was -43.7 mV while the zeta potential of PDDA-functionalized silica core particles (sample Cp) was $+54.9$ mV. The zeta potential of particles obtained by the deposition of silica nanoparticles generated at 80°C from the sodium silicate solution on the surface of positively charged silica core particles was -51.6 mV (sample CpS). This could indicate that the surface of PDDA-functionalized silica core particles was covered with a continuous silica layer. Lipase from *C. rugosa* was immobilized inside the mesoporous silica shell of the previously obtained silica core-shell particles (sample CpS), and then the support particles were functionalized with PDDA. The zeta potential of PDDA-functionalized silica core-shell particles (sample Cp-Sp) was $+39.1$ mV. Finally, to prevent enzyme leakage from the support, the silica nanoparticles generated at 40°C from the highly basic sodium silicate solution were deposited on the surface of PDDA-functionalized silica core-shell particles. The zeta potential of bilayered silica core-shell particles (sample Cp-Sp-S) was -33.4 mV, which might indicate that a continuous external silica layer was formed around monolayered silica core-shell enzyme support particles.

The average particle size distributions of silica core particles and monolayered and bilayered core-shell particles (samples C, Cp-S and Cp-Sp-S) are shown in Fig. 10. The average particle size distributions of these particles are approximately 450, 550 and 650 nm, respectively, which indicates increasing

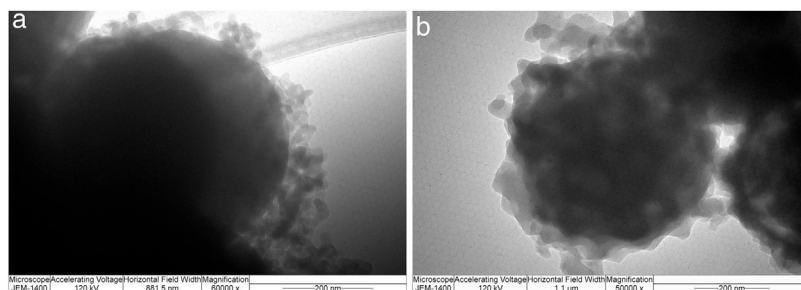


Fig. 9 – TEM micrographs of: (a) monolayered and (b) bilayered silica core-shell particles.

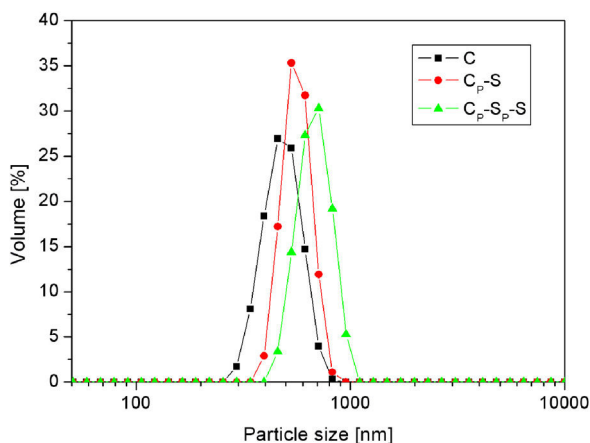


Fig. 10 – Particle size distributions of silica core (C) and core-shell particles (C_p -S and C_p -S_p-S).

of the particle size with successive deposition of two silica monolayers. The average thickness of the monolayered shell is ~ 50 nm, while the thickness of the bilayered shell is ~ 100 nm. The similar information was obtained by TEM analysis (Fig. 9).

The results of the hydrolysis of 4-nitrophenyl acetate (pNPA) into 4-nitrophenol released per gram of the monolayered silica core-shell material (sample C_p S) containing the immobilized lipase are shown in Table 2. As shown in Table 2, the monolayered silica core-shell particles containing the immobilized lipase showed a loss of activity after 10 reaction cycles by approximately six times. The highest activity was after the first cycle, and it was $4.92 \mu\text{mol}$ of 4-nitrophenol per gram of monolayered core-shell silica per minute. In other words, the activity of the immobilized lipase was $0.29 \mu\text{mol}$ of 4-nitrophenol released per milligram of the immobilized lipase per minute. The decrease in the activity of the material (sample C_p S) containing the immobilized lipase was probably due to the desorption of lipase from the monolayered silica shell. Conversely, the activity of the free enzyme obtained

under similar conditions (the initial substrate concentration of 1.1 mM and 25°C) was $29 \mu\text{mol}$ of 4-nitrophenol per milligram of lipase per minute. The activity of the immobilized lipase was lower than that of the free enzyme, probably due to diffusion limitations and the blockage of the enzyme's active site.

To prevent enzyme desorption from the mesoporous silica layer, an external mesoporous silica layer was formed by the deposition of silica nanoparticles generated by the neutralization of highly basic sodium silicate solution on the previously obtained silica core-shell particles (sample C_p S) containing the immobilized lipase.

The activity of bilayered silica core-shell particles (sample C_p -S_p-S) containing the immobilized lipase was approximately $0.166 \mu\text{mol/g min}$ ($0.166 \mu\text{mol}$ of 4-nitrophenol per gram of the silica material per minute). In other words, the activity of the immobilized lipase was $0.04 \mu\text{mol}$ of 4-nitrophenol per milligram of lipase per minute. The decreased activity of the lipase immobilized on the bilayered silica shell (sample C_p -S_p-S) relative to the lipase immobilized on the monolayered silica shell was probably due to mass transfer resistance in the external silica layer. The internal mass transfer resistance occurred in interstitial pores of external mesoporous silica layer as well as in thin PDDA layer surrounding internal mesoporous silica layer.

Immobilization of invertase in the mesoporous silica core-shell structure

To allow invertase immobilization inside the mesoporous silica layer, invertase was immobilized inside the simultaneously deposited silica layer (Fig. 11). SEM and TEM micrographs of the silica core-shell particles containing the immobilized invertase are presented in Fig. 12. As shown, a non-uniform shell was obtained since the reaction was prolonged until the gel point was reached to ensure the entrapment of each enzyme dissolved in the reaction vessel inside the mesoporous silica layer.

Table 2 – The activity of lipase immobilized on monolayered silica core-shell particles (sample C_p S) expressed as the amount of 4-nitrophenol released per gram of the support per minute.

	Number of cycles									
	I	II	III	IV	V	VI	VII	VIII	IX	X
Activity of immobilized lipase on sample C_p S [$\mu\text{mol/g min}$]	4.92	1.92	1.755	1.49	1.346	1.138	1.038	0.915	1	0.838

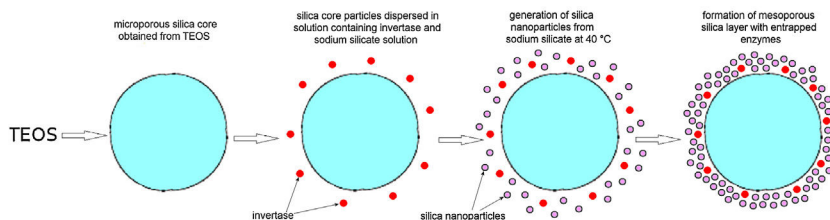


Fig. 11 – A schematic illustration of the preparation of silica core-shell particles containing immobilized invertase.

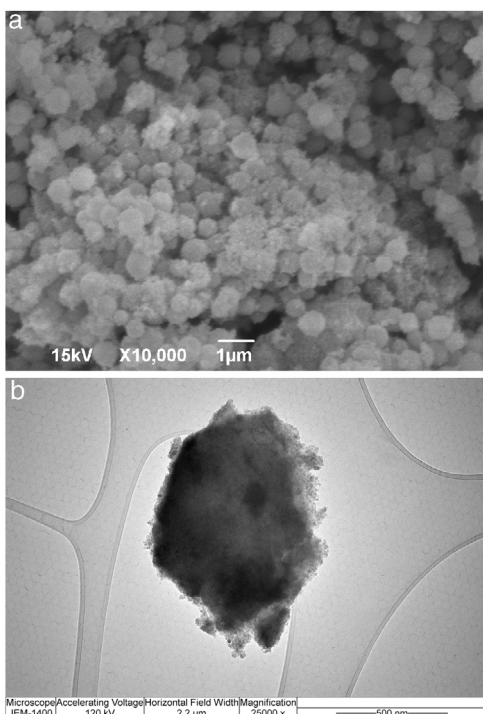


Fig. 12 – SEM and TEM micrographs of silica core-shell particles containing immobilized invertase.

The results about the gel point and network formation are summarized in Fig. 13. The results showed the viscosity change with change in shear rate for the starting sodium silicate solution (having a $\text{Na}_2\text{O}/\text{SiO}_2$ molar ratio of 0.28 and a SiO_2 concentration of 0.91 mol/l) and samples obtained by neutralization of sodium silicate solution at 70 °C and taken from vessel during the reaction at three different time intervals (300, 420 and 450 s), respectively. Sulfuric acid was slowly added into the well-stirred sodium silicate solution at 70 °C, so that the speed of neutralization was constant over the whole reaction time. The average viscosity of the starting sodium silicate solution was ~ 0.0012 Pa s (Fig. 13a). The viscosity was marginally changed after 300 s of reaction (Fig. 13a). Further prolongation of reaction time (420 s) resulted in a slight increase of viscosity (the average viscosity was about 0.0035 Pa s) (Fig. 13a). The viscosity of sodium silicate solution increased sharply after 450 s (the average viscosity was about 0.2 Pa s), indicating that the gel point was reached (Fig. 13b).

The results of sucrose hydrolysis catalyzed by invertase, either in a free form or immobilized on silica core-shell particles are presented in Table 3. The activities of the free and

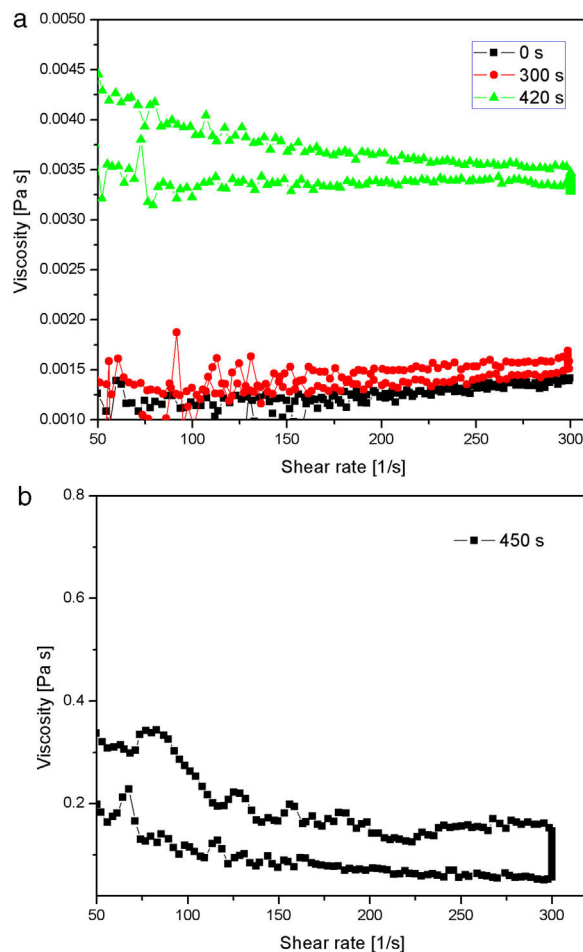


Fig. 13 – The viscosity change with change in shear rate: (a) starting sodium silicate solution (■), samples obtained by neutralization and taken from vessel after 300 s (●) and 420 s (▲); (b) sample obtained by neutralization and taken from vessel after 450 s (▼).

immobilized invertase were measured at three sucrose concentrations (0.05, 0.1 and 0.2 mol/l). The activity of invertase was shown as the amount of inverted sugar (micromoles) released per microgram of invertase after one hour of incubation. The activity of the immobilized invertase was shown as the amount of inverted sugar (micromoles) released per microgram of the immobilized invertase after one hour of incubation.

As shown in Table 3, the activity of the free invertase gradually decreased with increasing sucrose concentration. This indicates that the free enzyme was subject to substrate

Table 3 – The activity of free and immobilized invertase at three sucrose concentrations.

	Sucrose concentration [mol/l]		
	0.05	0.1	0.2
Free invertase [$\mu\text{mol}/\mu\text{g h}$]	9	8.535	5.629
Immobilized invertase [$\mu\text{mol}/\mu\text{g h}$]	0.016	0.0608	0.4752

inhibition at the sucrose concentrations used. The activity of the immobilized invertase gradually increased until the sucrose concentration reached 0.1 mol/l. Then, the activity rate rose rapidly when the sucrose concentration reached 0.2 mol/l. This indicates that mass transfer resistance for the substrate to the enzyme active site was present inside the mesoporous silica layer and affected the effectiveness of the immobilized invertase. The mass transfer rate was lower at a low sucrose concentration and increased with increasing sucrose concentration.

Conclusion

A continuous monolayered mesoporous silica shell with average thickness of ~ 60 nm was formed by deposition of silica nanoparticles generated at 80°C from highly basic sodium silicate solution on the surface of PDDA-functionalized silica core particles (having an average size of ~ 400 nm). The average pore size of the monolayered silica shell was ~ 24 nm, which allowed lipase immobilization inside mesoporous silica layer. The immobilization efficiency of lipase on the mesoporous silica layer was 80%. The activity of the immobilized lipase was lower than that of the free enzyme due to diffusion limitations and the blockage of the active site. Moreover, the activity of the heterogeneous biocatalyst decreased six times through the ten reaction cycles due to lipase leakage from the monolayered shell. To prevent lipase leakage from the support, an outer mesoporous silica layer was deposited at a lower temperature (40°C) on the surface of PDDA-functionalized silica core-shell particles containing the immobilized lipase. The deposition of the second layer was performed at a relatively lower temperature to prevent thermal inactivation of the immobilized enzyme. The average shell thickness and pore size of the outer silica layer was ~ 60 nm and 17 nm, respectively. The reaction time necessary for deposition of outer and internal silica layers was 12 and 9 min, respectively, indicating that an increase of reaction temperature increased the tendency for deposition of silica nanoparticles on the PDDA-functionalized silica surface. The activity of the lipase immobilized inside the bilayered shell was further reduced due to diffusion resistance within the outer silica layer and PDDA layer placed between two silica layers however, it was retained for the next reaction cycles.

When a similar procedure was used for the immobilization of invertase onto the monolayered mesoporous silica layer, the efficiency was 0%. The reason was the larger invertase size compared to actual pore size of mesoporous silica monolayer. Therefore, another procedure was developed for the immobilization of invertase in the mesoporous silica layer. It involved the dissolution of invertase in a dispersion of PDDA-functionalized silica core particles and silica nanoparticles generated at 40°C from sodium silicate solution. To allow completely enzyme immobilization, invertase was entrapped

by in situ gelling silica system. The immobilized invertase showed lower activity than the free enzyme, but its activity was not hampered by the inhibition of the substrate at its higher concentrations due to the location of the enzyme inside the mesoporous silica layer, where the mass transfer resistance for the substrate to the enzyme active site was present.

Further research will focus on increasing the activity of the enzymes immobilized inside the mesoporous silica shell.

Uncited references

[14,22].

Acknowledgments

This work was financially supported by the Ministry of Education, Science and Technological Development of the Republic of Serbia under Project OI 172057 and Project III45021

REFERENCES

- [1] O.F. Brandenburg, C.K. Prier, K. Chen, A.M. Knight, Z. Wu, F.H. Arnold, Stereoselective enzymatic synthesis of heteroatom-substituted cyclopropanes, *ACS Catal.* 8 (2018) 2629–2634, <http://dx.doi.org/10.1021/acscatal.7b04423>.
- [2] J. Mu, J. Lin, P. Huang, X. Chen, Development of endogenous enzyme-responsive nanomaterials for theranostics, *Chem. Soc. Rev.* 47 (2018) 5554–5573, <http://dx.doi.org/10.1039/C7CS00663B>.
- [3] D.R. Bagal-Kestwal, M.H. Pan, B.-H. Chiang, Electrically nanowired-enzymes for probe modification and sensor fabrication, *Biosens. Bioelectron.* 121 (2018) 223–235, <http://dx.doi.org/10.1016/j.bios.2018.09.018>.
- [4] V.K. Nathan, M.E. Rani, R. Gunaseeli, N.D. Kannan, Enhanced biobleaching efficacy and heavy metal remediation through enzyme mediated lab-scale paper pulp deinking process, *J. Clean. Prod.* 203 (2018) 926–932, <http://dx.doi.org/10.1016/j.jclepro.2018.08.335>.
- [5] F. Pitzalis, M. Monduzzi, A. Sali, A bienzymatic biocatalyst constituted by glucose oxidase and horseradish peroxidase immobilized on ordered mesoporous silica, *Micropor. Mesopor. Mater.* 241 (2017) 145–154, <http://dx.doi.org/10.1016/j.micromeso.2016.12.023>.
- [6] N.B. Carvalho, B.T. Vidal, A.S. Barbosa, M.M. Pereira, S. Mattedi, L.S. Freitas, A.S. Lima, M.F. Cleide, C.M.F. Soare, Lipase immobilization on silica xerogel treated with protic ionic liquid and its application in biodiesel production from different oils, *Int. J. Mol. Sci.* 19 (2018) 1829–1848, <http://dx.doi.org/10.3390/ijms19071829>.
- [7] R. Hayes, A. Ahmed, T. Edge, H. Zhang, Core-shell particles: preparation, fundamentals and applications in high performance liquid chromatography, *J. Chromatogr. A* 1357 (2014) 36–52, <http://dx.doi.org/10.1016/j.chroma.2014.05.010>.

- [8] A.M. Mebert, C. Aime, G.S. Alvarez, Y. Shi, S.A. Flor, S.E. Lucangioli, M.F. Desimone, T. Coradin, Silica core-shell particles for the dual delivery of gentamicin and rifamycin antibiotics, *J. Mater. Chem. B* 4 (2016) 3135–3144, <http://dx.doi.org/10.1039/C6TB00281A>.
- [9] G.H. Jeong, E.G. Kim, S.B. Kim, E.D. Park, S.W. Kim, Fabrication of sulfonic acid modified mesoporous silica shells and their catalytic performance with dehydration reaction of D-xylose into furfural, *Micropor. Mesopor. Mater.* 144 (2011) 134–139, <http://dx.doi.org/10.1016/j.micromeso.2011.04.002>.
- [10] E. Poorakbar, A. Shafiee, A.A. Saboury, B.L. Rad, K. Khoshnevisan, L. Ma'mani, H. Derakhshankhah, M.R. Ganjal, M. Hosseini, Synthesis of magnetic gold mesoporous silica nanoparticles core shell for cellulase enzyme immobilization: improvement of enzymatic activity and thermal stability, *Process. Biochem.* 71 (2018) 92–100, <http://dx.doi.org/10.1016/j.procbio.2018.05.012>.
- [11] W. Stöber, A. Fink, E. Bohn, Controlled growth of monodisperse silica spheres in the micron size range, *J. Colloid Interface Sci.* 26 (1968) 62–69, [http://dx.doi.org/10.1016/0021-9797\(68\)90272-5](http://dx.doi.org/10.1016/0021-9797(68)90272-5).
- [12] G. Buchel, M. Gurnn, K.K. Unger, A. Matsumoto, K. Tsutsumi, Tailored synthesis of nanostructured silica: control of particle morphology, particle size and pore size, *Supramol. Sci.* 5 (1998) 253–259, [http://dx.doi.org/10.1016/S0968-5677\(98\)00016-9](http://dx.doi.org/10.1016/S0968-5677(98)00016-9).
- [13] R. Filipović, Z. Obrenović, I. Stijepović, Lj.M. Nikolić, V.V. Srdić, Synthesis of mesoporous silica particles with controlled pore structure, *Ceram. Int.* 35 (2009) 3347–3353, <http://dx.doi.org/10.1016/j.ceramint.2009.05.040>.
- [14] J. Allouche, J.-C. Dupin, D. Gonbeau, Generation of a mesoporous silica MSU shell onto solid core silica nanoparticles using a simple two-step sol-gel process, *Chem. Commun.* 47 (2011) 7476–7478, <http://dx.doi.org/10.1039/C1CC12242H>.
- [15] M.D. Sacks, K. Wang, G.W. Scheiffele, N. Bozkurt, Effect of composition on mullitization behavior of α -alumina/silica microcomposite powders, *J. Am. Ceram. Soc.* 80 (3) (1997) 663–672, <http://dx.doi.org/10.1111/j.1151-2916.1997.tb02882.x>.
- [16] M.P. Nikolić, K.P. Giannakopoulos, M. Bokorov, V.V. Srdić, Effect of surface functionalization on synthesis of mesoporous silica core-shell particles, *Micropor. Mesopor. Mater.* 155 (2012) 8–13, <http://dx.doi.org/10.1016/j.micromeso.2011.12.046>.
- [17] M.P. Nikolić, R. Filipović, S. Stanojević-Nikolić, Effect of reaction time on formation of silica core-shell particles, *Process. Appl. Ceram.* 9 (2015) 209–214, <http://dx.doi.org/10.2298/PAC1504209N>.
- [18] E. Jeong, G. Lee, S.W. Han, W.J. Lee, H.S. Choi, Y. Lee, J.W. Kim, Polyelectrolyte/silica-layered hydrogel microcapsules as vehicles with remarkable shell impermeability, *J. Ind. Eng. Chem.* 46 (2017) 192–198, <http://dx.doi.org/10.1016/j.jiec.2016.10.030>.
- [19] S. Benjamin, A. Pandey, *Candida rugosa* lipases: molecular biology and versatility in biotechnology, *Yeast* 14 (1998) 1069–1087, [https://doi.org/10.1002/\(SICI\)1097-0061\(19980915\)14:12<1069::AID-YEA303>3.0.CO;2-K](https://doi.org/10.1002/(SICI)1097-0061(19980915)14:12<1069::AID-YEA303>3.0.CO;2-K).
- [20] S. Gao, Y. Wang, X. Diao, G. Luo, Y. Dai, Effect of pore diameter and cross-linking method on the immobilization efficiency of *Candida rugosa* lipase in SBA-15, *Bioresour. Technol.* 101 (2010) 3830–3837, <http://dx.doi.org/10.1016/j.biortech.2010.01.023>.
- [21] Sigma-Aldrich, Product Information, 2013, <https://www.sigmaaldrich.com/content/dam/sigma-aldrich/docs/Sigma/Product.Information.Sheet/2/i4504pis.pdf>.
- [22] M. Bradford, A rapid and sensitive method for the quantitation of microgram quantities of protein utilizing the principle of protein-dye binding, *Anal. Biochem.* 72 (1976) 248–254, [http://dx.doi.org/10.1016/0003-2697\(76\)90527-3](http://dx.doi.org/10.1016/0003-2697(76)90527-3).
- [23] S. Brunauer, P.H. Emmett, E. Teller, Adsorption of gases in multimolecular layers, *J. Am. Chem. Soc.* 60 (1938) 309–319, <http://dx.doi.org/10.1021/ja01269a023>.
- [24] E.P. Barrett, L.G. Joyner, P.P. Halenda, The determination of pore volume and area distributions in porous substances. I. Computations from nitrogen isotherms, *J. Am. Chem. Soc.* 73 (1951) 373–380, <http://dx.doi.org/10.1021/ja01145a126>.
- [25] H. Gustafsson, C. Thorn, K. Holmberg, A comparison of lipase and trypsin encapsulated in mesoporous materials with varying pore sizes and pH conditions, *Colloid. Surf. B* 87 (2011) 464–471, <http://dx.doi.org/10.1016/j.colsurfb.2011.06.012>.
- [26] G.L. Miller, Use of dinitrosalicylic acid reagent for determination of reducing sugar, *Anal. Chem.* 31 (1959) 426, <http://dx.doi.org/10.1021/ac60147a030>.